Effects of the copper oxide nanoparticles (CuO NPs) on *Galleria mellonella* hemocytes

A. Eskin & Hakan Bozdoğan

Published online: 03 Mar 2021.

Submit your article to this journal ⏎

View related articles ⏎

View Crossmark data ⏎

Taylor & Francis
Taylor & Francis Group

RESEARCH ARTICLE

Effects of the copper oxide nanoparticles (CuO NPs) on *Galleria mellonella* hemocytes

A. Eskin[a] and Hakan Bozdoğan[b]

[a]Department of Crop Animal Production, Avanos Vocational School, University of Nevşehir Hacı Bektaş Veli, Nevşehir, Turkey; [b]Department of Plant and Animal Production, Vocational School of Technical Sciences, University of Kırşehir Ahi Evran, Kırşehir, Turkey

ABSTRACT

In this study, 38 nm-sized and flake-like-shaped CuO NPs (10, 50, 100, 150 µg/10 µl/larva) were force-fed to fourth instar (100 ± 20 mg) *Galleria mellonella* (Lepidoptera: Pyralidae) larvae under the laboratory conditions. The effects of CuO NPs on total hemocyte counts (THCs) and the frequency of viable, mitotic, apoptotic, necrotic, and micronucleated hemocyte indices were detected with the double-staining protocol by hematoxylin and eosin (H&E) stains. The total hemocyte counts (THCs) did not change significantly in *G. mellonella* larvae at all concentrations for 24 h and 72 h post-force-feeding treatment. The ratio of viable hemocytes decreased at 50, 100, 150 µg/10 µl concentrations in 24 h and 72 h when compared with untreated larvae. The increases in the percentage of mitotic and micronucleated hemocytes were statistically significant at 150 µg/10 µl in 24 h. The results showed that high concentrations (>10 µg/10 µl) of CuO NPs increased the percentage of apoptotic hemocytes in 24 h. 100 and 150 µg/10 µl of CuO NPs caused a significant increase in the percentage of necrotic hemocytes in 24 h. The decrease in the percentage of mitotic hemocytes at 10, 100 and 150 µg/10 µl in 72 h was statistically significant. Apoptotic hemocytes increased and were found to be higher at 100 and 150 µg/10 µl of CuO NPs in 72 h in comparison with the untreated larvae. Finally, we observed an increase in the percentage of necrotic hemocytes at 150 µg/10 µl in 72 h.

Introduction

In recent years, nanoparticles (NPs) have been introduced to a wide range of biological applications used in the medical industry, against cancer, neurological disorders, cardiovascular diseases, respiratory disorders, liver diseases and skin infections (Rai *et al*. 2015). Also, NPs are being used for diverse purposes, from medical treatments and energy storage in various branches of industrial products such as solar and oxide fuel batteries for energy storage, to wide incorporation into diverse materials of everyday use such as cosmetics or clothes (Hasan 2015, Jeevanandam *et al*. 2018). For a metallic particle to be considered 'Nano,' its size must be between 1–100 nm (Nakamura *et al*. 2019). Copper oxide nanoparticles (CuO NPs) are used today in many fields such as commercial products, agrochemicals, paints, semiconductor compounds, sensors, catalyzers, and antimicrobial products, which leads to their growing release into terrestrial and aquatic ecosystems (Keller *et al*. 2017, Simonin *et al*. 2018, Tunçsoy 2018). The CuO belongs to the monoclinic crystal system, with a crystallographic point group of 2/m or C_{2h-} (Sahdan *et al*. 2015). Its monoclinic structure offers thermal superconductivity, thermal stability (Zhang *et al*. 2014, Quirino *et al*. 2018), photovoltaic properties, and antimicrobial activity to CuO nanostructue (Tran and Nguyen 2014, Quirino *et al*. 2018). Today, living organisms can be exposed

to nanomaterials that are present in the environment. As a result, determining the negative effects of nanomaterials on biological systems is one of the research topics. In addition to this exposure, the physicochemical properties of NPs are very important in the evaluation of toxic effects. For example, the unique size, shape, morphology, composition, distribution, dispersion, surface area, surface chemistry, and reactivity of nanomaterials are expected to affect their toxicity (Oberdorster *et al*. 2005, Sahu and Hayes 2017), which makes their toxicity evaluation complex (Dhawan and Sharma 2010, Pfaller *et al*. 2010, Sahu and Hayes 2017). NPs can have different shapes and sizes such as, nanospheres, nanorods, nanobars, nanoprisms, decahedron by selecting different chemicals during their synthesis for reduction and stabilization of them (Mukherji *et al*. 2019). CuO NPs can be in needle, spherical, spindle, sheet, flake, and nanowire shapes (Eltarahony *et al*. 2018). The specific characteristics of nanomaterials determine their toxicity in higher organisms (Brandelli, 2020). Due to their physical and chemical properties, NPs may be more toxic to organisms than ionic forms. In addition, they can enhance the enzymatic antioxidant defence system, DNA damage, membrane permeability, cell death, and cause the genotoxicity and neurotoxicity in organisms (Tunçsoy, 2018). CuO NPs induce reactive oxygen species (ROS) and oxidative stress, which can cause DNA

CONTACT A. Eskin ataeskin@nevsehir.edu.tr Department of Crop Animal Production, Avanos Vocational School, University of Nevşehir Hacı Bektaş Veli, Nevşehir, Turkey

damage and increase the expression of death receptors (Yang et al. 2009, Shafagh et al. 2015). Under physiological and pathological conditions, both reactive oxygen species (ROS) and mitochondria play an important role in the induction of apoptosis (Simon et al. 2000). Cells may activate the controlled cell death (apoptosis) program, or necrosis may occur where the membrane integrity is lost and uncontrolled death is being executed for cell lysis. The CuONP-treated cell can die by apoptosis and necrosis, which can be distinguished by morphological and biochemical features (Alarifi et al. 2013). Evidence of necrosis with nuclear lysis, organelle disintegration, cytoplasm vacuolation, and intercellular contact disorganization was indeed observed after topical application of CuO NPs onto stripped, but not intact, epidermis (Alarifi et al. 2013). Cuo NP-based cytotoxicity in keratinocytes and fibroblasts has also been reported in the literature (Alarifi et al. 2013, Luo et al. 2014). Conversely, the cells exposed to the process of necrosis commonly swell rapidly, lose membrane integrity, stopped metabolism, and secreted their contents (İstifli et al. 2019). Damaged cells undergoing necrosis display gross morphological and anatomical structures when exposed to extreme environmental conditions, which is different from apoptosis in almost every respect (Ferri and Kroemer 2001). Mitotic index, which means the relative number of hemocytes in the total cell population and its alterations helps to determine the cytotoxic effects of an agent (Beaulaton 1979, Vieira and Silveria 2018). Micronucleus structures can arise from the mitotic loss of acentric fragments, a variety of consequences of chromosomal breakage, an exchange or mitotic loss of chromosomes, and apoptosis. The second is a form of nuclear destruction where the nucleus disintegrates and nuclear fragments are formed (Koç-Başer et al. 1999, Tomanin 1991). The micronucleus test is frequently used to determine the genotoxic effects of various chemicals, chemical compounds, and agrochemicals on organisms (Hayashi 2016). The cytotoxic, genotoxic effects and potential toxicity values of some chemical compounds on some insects were investigated by force-feeding treatment (Dere et al. 2015, Eskin et al. 2019, Gwokyalya et al. 2019, Eskin et al. 2020). Force-feeding is the practice of forcing a person or an animal to eat and drink, often by putting food into the stomach through the mouth by means of a pipe. The toxicity studies of microorganisms or toxic substances are carried out on insects via forced-feeding treatment (Ramarao et al. 2012, Dere et al. 2015, Eskin et al. 2019). One model organism that has been utilized for studies on cytotoxicology of nanomaterials is the greater wax moth Galleria mellonella (Lepidoptera: Pyralidae). The caterpillar larva of the greater wax moth G. mellonella has several advantages, including the ability to incubate at 37 °C, short life span, and a size that is convenient for handling and relatively precise dosing (Andrea et al. 2019). The immune system of G. mellonella larvae is structurally and functionally similar to the innate immune response of mammals, which makes this model suitable for such studies (Pereira et al. 2018). Therefore, nanotoxicology-based studies with this insect will help determine the possible effects on the ecosystem and humans (Zorlu et al. 2018). The negative effects of CuO NPs on enzyme activity such as and catalase (CAT),

superoxide dismutase (SOD), glutathione peroxidase (GPx), glutathione-s-transferase (GST), acetylcholinesterase (AChE) by increasing ROS levels have also been reported in G. mellonella larvae (Tunçsoy et al. 2019). However, studies to determine the toxic effects of CuO NPs on G. mellonella hemocytes are quite limited. So, we conducted the present study to determine whether 38 nm-sized and flake-like-shaped CuO NPs affect the THCs of G. mellonella. Besides, the various identified effects, it is possible that CuO NPs affects the cellular immunity of insects and to reveal these effects, different cell staining methods are used to detect viable, apoptotic, necrotic, mitotic, and micronucleated cells. Ou et al. (2014) identified cell apoptosis with Wright-Giemsa staining. They found that EPSAH treatment to Hela cells (50–800 μg/ml for 48 h) showed nuclear fragmentation, chromatin condensation and/or chromatin margination which were characteristic morphological alterations associated with apoptosis. In another study, apoptotic cells of the gingival epithelium were detectable after using hematoxylin and eosin staining (Nayak et al. 2016).

In this study, we stained the G. mellonella hemocytes with a hematoxylin and eosin staining method, and we observed the apoptotic bodies and the condensation of the nucleus clearly. Then, we studied apoptotic, necrotic, mitotic, micronucleated indices of the circulating larval hemocytes of G. mellonella to reveal the cytotoxic effects of CuO NPs.

Materials and methods

Insects

Galleria mellonella at different life stages (larvae and pupae) were provided by beekeepers in Nevşehir Province, Turkey. Larvae of G. mellonella were collected from infested beehives and reared in jars (1 l capacity) until the emergence of the moths. Their laid eggs were collected. The rearing was carried out using natural wax. The insect colony consisting of control (untreated) and experiment groups (NP treated) were reared in dark conditions at 26 ± 3 °C with 60 ± 5% relatively humidity. All insects rearing and toxicity studies of NPs were carried out at Avanos Vocational School of Higher Education, Avanos, Nevşehir, Turkey. Fourth instar (100 ± 20 mg) G. mellonella (Rahman et al. 2017) larvae were used in all experiments.

Chemicals and materials

In this study, 38 nm-sized and flake-like-shaped CuO NPs were used. It is a nanopowder and a commercial product of Nanokar (Istanbul/TURKEY). Hematoxylin (400. ZA. CB 6601) and Eosin Y (400. ZA. CB 2396) stains were purchased from Zag Chemistry (Istanbul/TURKEY). Distilled water, 29 gauges micro-fine insulin syringe, light microscope (Olympus CX21, Japan), 70% ethyl alcohol, cotton, bath type sonicator (Isolab, TURKEY), honeycomb, 20 ml plastic boxes, and hematoxylin (400. ZA. CB 6601) and Eosin Y (400. ZA. CB 2396) stains were used in all experiments. Luna automated cell counter (USA) and Luna cell counting slide (USA) were used for total hemocyte counting of G. mellonella larvae. The microscopic images

of hemocytes were taken at magnifications of 1000× with a Swift microscope camera (USA). Olympus CH2 (Japan) light microscope was used to take pictures of hemocytes with a Swift microscope camera.

Characterization of CuO NPs

The scanning electron microscope (SEM) analysis of CuO NPs was examined at the Erciyes University Nanotechnology Research Center (ERNAM). A gold coating was applied using a sputter coating machine (Quorum, Q150R ES, UK) to overcome the non-conductive nature of the material. The images of the CuO NPs were taken by scanning electron microscopy using a Zeiss EVO 50 LS10 (Germany) at 25 kV. The scanning transmission electron microscope (FESEM) analysis of CuO NPs was conducted at the Erciyes University Technology Research and Application Center (TAUM). The morphology of the CuO NPs was investigated by field emission scanning electron microscopy (FESEM) analysis. The images of the CuO NPs were taken by using a Zeiss GEMINI 500 device which was connected to FESEM detector at 25 kV. X-ray powder diffraction (XRD) analysis of CuO NPs was examined at Marmara University, Faculty of Engineering, Metallurgical and Materials Engineering Department with reference code 98-002-8662.

Determination of lethal concentration 50 and 90 (LC$_{50}$ and LC$_{90}$) values of CuO NPs in G. mellonella larvae

The toxicity test protocol was arranged according to Ramarao et al. (2012), Altuntaş et al. (2016), and Eskin et al. (2019). CuO NPs were dissolved in distilled water to prepare a stock solution of μg/10 μl. The concentrations of CuO NPs (1, 10, 100, 1000 μg/10 μl/larva) were prepared from the stock solution to determine the acute toxicity on larvae for 24 h and 72 h. Distilled water free from CuO NPs was used as a control treatment. After the dissolution of CuO NPs in distilled water, suspension was homogenized by a bath-type sonicator for 10 min at 40 °C. Totally, 60 (three replicates, each replicate consisted of 20 larvae) fourth instar larvae (100 ± 20 mg) were used for every treatment (control and for each experiment groups). The selected fourth instar larvae were starved for 3 h (Dere et al. 2019). CuO NPs were administered to the larvae by the force-feeding method. The force-feeding treatment of CuO NP concentrations to the larvae was carried out according to (Ramarao et al. 2012, Eskin et al. 2019).

Force-feeding treatment

Larvae (100 ± 20 mg) were force-fed with 10 μl of the homogenized CuO NPs concentrations (1, 10, 100, 1000 μg/10 μl/larva) or 10 μl distilled water with a micro-fine insulin syringe (29 gauges) under the stereomicroscope (Ramarao et al. 2012, Eskin et al. 2019). The needle was sterilized with ethyl alcohol (70%) and cotton after each larva force-fed. Post-force-feeding treatment, each larva was kept in a sterile plastic box (20 ml, with 20 pinhole holes on the top cover to allow necessary air circulation) without natural wax in dark

conditions at 26 ± 3 °C with 60 ± 5% relatively humidity. The numbers of dead larvae and the numbers of viable larvae were counted in 24 and 72 h for probit analysis. The lethal concentrations (LC$_{50}$ and LC$_{90}$ values) of CuO NPs on the fourth instar G. mellonella larvae were determined by probit analysis using IBM-SPSS (2011) software (IBM, NY, USA) with 95% confidence levels at 24 and 72 h. According to LC$_{50}$ values of CuO NPs, 10, 50, 100, 150 μg/10 μl CuO NPs concentrations were determined as experimental (treated) concentrations for all hemocyte studies. The larvae were force-fed with the suspension of CuO NPs at concentrations of 10, 50, 100, and 150 μg/10 μl/larva or 10 μl distilled water (control group, 0) (Ramarao et al. 2012, Altuntaş et al. 2016 and Eskin et al. 2019).

Total hemocyte counting (THC) in the automated cell counter

The cytotoxic effects of CuO NPs on larval G. mellonella hemocytes for 24 and 72 h were studied. The experiments were performed according to the following steps for each larva. Firstly, 45 μl anticoagulant PBS (0.098 M NaOH, 0.186 M NaCl, 0.017 M Na$_2$EDTA and 0.041 M citric acid, pH 4.5) was added into the centrifuge tube. A fine insect needle was used to drill the larvae from the anterior section of the hind leg to collect hemolymph. 5 μl of larval hemolymph was taken with a micropipette. This amount of hemolymph was transferred into the Eppendorf tube containing 45 μl PBS. Then, the mixture of PBS and hemolymph was homogenized with a micropipette. 10 μl of hemolymph was withdrawn with a micropipette and applied to the Luna cell counting slide. Finally, the hemocyte size protocol was set in the Luna automated cell counter device as follows: minimum cell size 5 μm, maximum cell size 40 μm, dilution factor: 10. The number of hemocytes per cubic millimeter (1 mm^3) in the hemolymph (THC) and hemocyte numbers in the 10 μl of the mixture (PBS + hemolymph) were counted in the device (Neuwirth 1973, Eskin et al. 2019). Five larvae were examined for each experimental group and replicated three times.

Evaluation of viable, apoptotic, necrotic, and micronucleated hemocytes

The dye-staining steps of the insect hemocytes were carried out at room temperature (26 °C) based on (Richardson et al. 2018) as follows.

Larvae were cleaned with a (70%) ethanol impregnated moist sterile piece of cloth for preparing slides. Larvae were drilled from the first segment on the back of the head by a fine needle, and 5 μl hemolymph was taken by a micropipette. Hemolymph was smeared onto clean and dry slide immediately. Then hematoxylin and eosin protocol was applied. The slides were washed in running tap water for 1 min. Finally, the slides dried for 10 min. at room temperature, and then they mounted on a coverslip with entellan. 1000 hemocytes were randomly selected in each slide. Each slide was scanned under a light microscope (Olympus CX21, Japan) at a magnification of 1000×. Five larvae were examined for each experimental group

and replicated three times. Viable, apoptotic, necrotic, mitotic, and micro-nucleated hemocytes were counted. The cell that has a fairly intact structure with a staining intensity was evaluated and accepted as a viable hemocyte. The cell that retained its color and was smaller than the main nucleus was evaluated and counted as micronucleated hemocyte (Venier et al. 1997). Necrotic hemocytes were evaluated and characterized by a pale cytoplasm and a large number of vacuoles, mainly in the cytoplasm and sometimes in the nucleus (Bolognesi 2019). Apoptotic hemocytes were evaluated and characterized by show chromatin condensation in the first stages and nuclear fragmentation into small nuclear bodies in the last stages, and their cytoplasm had a lower staining intensity compared with a viable hemocyte (Bolognesi 2019). Finally, the percentages of viable hemocytes, mitotic hemocytes, apoptotic hemocytes, necrotic hemocytes, and micronucleated hemocytes were calculated separately, and the significance levels of differences between the control and experimental groups were determined.

Statistical analysis

IBM-SPSS (Version 20.0 for Windows, SPSS Science, Chicago, IL, USA) was used for the data analysis. The Kruskal–Wallis test was used when the assumptions of one-way ANOVA were not met. Inter-group differences in the total hemocyte counts (THCs) were tested using the non-parametric Mann–Whitney U-test, with significance accepted at p values < 0.05. An arcsine square root transformation was performed on the percentages of viable, mitotic, apoptotic, necrotic, and micronucleated cells before the statistical analysis. Inter-group differences in the percentages of viable, mitotic, apoptotic, necrotic, and micronucleated cells were tested using the Mann–Whitney U-test, with significance accepted at p values < 0.05 (Altuntaş et al. 2012, Eskin et al. 2019).

Results

Figure 1 displays the SEM and FESEM images of CuO NPs below. The SEM images showed that CuO NPs were in a flake-like morphology (Figure 1(a,b)) (Reddy et al. 2012). The FESEM images confirm the nano-flake shapes of CuO NPs. The nano-flakes are densely populated (Figure 1(c,d)).

As is well-known, XRD is one of the main techniques used by mineralogists and solid-state chemists to examine the physical and chemical composition of unknown materials. It is a very important characterization tool in solid-state chemistry and materials science (Hassan et al. 2012). The XRD results showed that CuO NPs (Yankson et al. 2019) (Table 1) matched by (Foley 2018) with tenorite-pure monoclinic. The XRD patterns show that all of the diffraction peaks are in good agreement with the standard diffraction data for CuO (ICSD Number: 98-002-8662), and no characteristic peaks were observed for other oxides (such as Cu_2O or Cu_2O_3) (Figure 2). The peaks are broadening due to the nano-size effect (Shaffiey et al. 2014). Peaks for CuO NPs appear at $2\theta = 32.50$ (110), 35.52 (002), 38.67 (111), 48.76 (202), 53.53 (020), 58.05 (202), 61.56 (213), 66.03 (022), 67.98 (220), 72.12

(311), and 75.11 (303) respectively (Table 1 and Figure 2). Peak values correspond with the different planes of monoclinic phase of CuO NPs previously reported by literature studies (Bouazizi et al. 2015, Chikkanna et al. 2018) (Table 1 and Figure 2). The XRD Figure 2 shows the CuO NPs at 2-theta degree at 35.5° and 38.67° which belong to (002) and (111), respectively. The peaks confirmed that the studied nanomaterial is CuO NPs and has monoclinic structure. Its monoclinic structure means that it is a unique monoxide compound (Bouazizi et al. 2015).

LC_{50} and LC_{90} values were calculated to be 370.951 (μg/10 μl) and 781.709 (μg/10 μl) for 24 h and 298.22 (μg/10 μl) and 671.693 (μg/10 μl) for 72 h (Table 2). According to LC_{50} values of CuO NPs, 10, 50, 100, 150 μg/10 μl CuO NPs concentrations were determined as experimental (treated) concentrations in this study.

We observed and counted the viable, apoptotic, necrotic, mitotic, and micro-nucleated hemocytes. They were observed for the applied concentrations and imaged under a light microscope (Olympus CH2, Japan) at magnifications of 1000 x with a Swift microscope camera (USA) (Figure 3). The results of the mean number of hemocytes counted in Luna cell counting slide and the mean number of hemocytes in 1 ml fourth instar G. mellonella larva counted by Luna II automated cell counter are presented in Table 3 below. The 24 h exposure of fourth instar G. mellonella larvae to 10, 50, 100, and 150 μg of CuO NPs resulted in insignificant fluctuations in the number of hemocytes at 24 h that were 745.46 ± 85.77, 699.60 ± 92.72, 998 ± 102.90 for the control group and the 10 and 100 μg of CuO NPs groups, respectively (Kruskal–Wallis test $p > 0.05$, chi-square $= 7.168$, $p = 0.127$). The total hemocyte count/ml was 17.72 ± 1.71, 16.80 ± 4.41, 23.72 ± 3.15 for the control group and the 10 and 100 μg of CuO NPs groups, respectively. However, statistically significant differences were observed between the experimental groups. The mean number of hemocytes obtained from larvae force-fed with 100 μg CuO NPs (998, 23.72×10^6/ml) was higher than the group force-fed with 10 μg CuO NPs (699.60, 16.80×10^6) group (Mann–Whitney U-test $p < 0.05$, $df = 4$, $p = 0.00$) (Table 3). Furthermore, 72 h post-force-fed larvae showed fluctuations in the mean hemocyte count between 617 (150 μg/10 μl CuO NPs)-1036 (50 μg CuO NPs) and 14.96×10^6 (150 μg CuO NPs)-24.40×10^6 (50 μg CuO NPs) (total hemocyte count/ml) in the hemolymph (Table 2). But these means were not statistically significant when compared to the control group (Kruskal–Wallis test $p > 0.05$, chi-square $= 6.736$, $p = 0.151$) (Table 3). The results of the percentages of viable hemocytes, mitotic hemocytes, apoptotic hemocytes, necrotic hemocytes, and micronucleated hemocytes are presented in Table 4 below.

The ratio of viable hemocytes decreased significantly at 50, 100, and 150 μg at 24 h and 72 h when compared with untreated larvae. 24 h post-force-feeding treatment of the CuO NPs, a 1.89 fold increase of the percentage of mitotic hemocytes at 150 μg ($F = 9.75$, $df = 4$, $p = 0.00$), and a 4.97 fold increase of the percentage of micro-nucleated hemocytes at the same concentration were statistically significant ($F = 11.76$, $df = 4$, $p = 0.00$) when compared to the control group (Table 4). 50, 100, and 150 μg of CuO NPs caused a
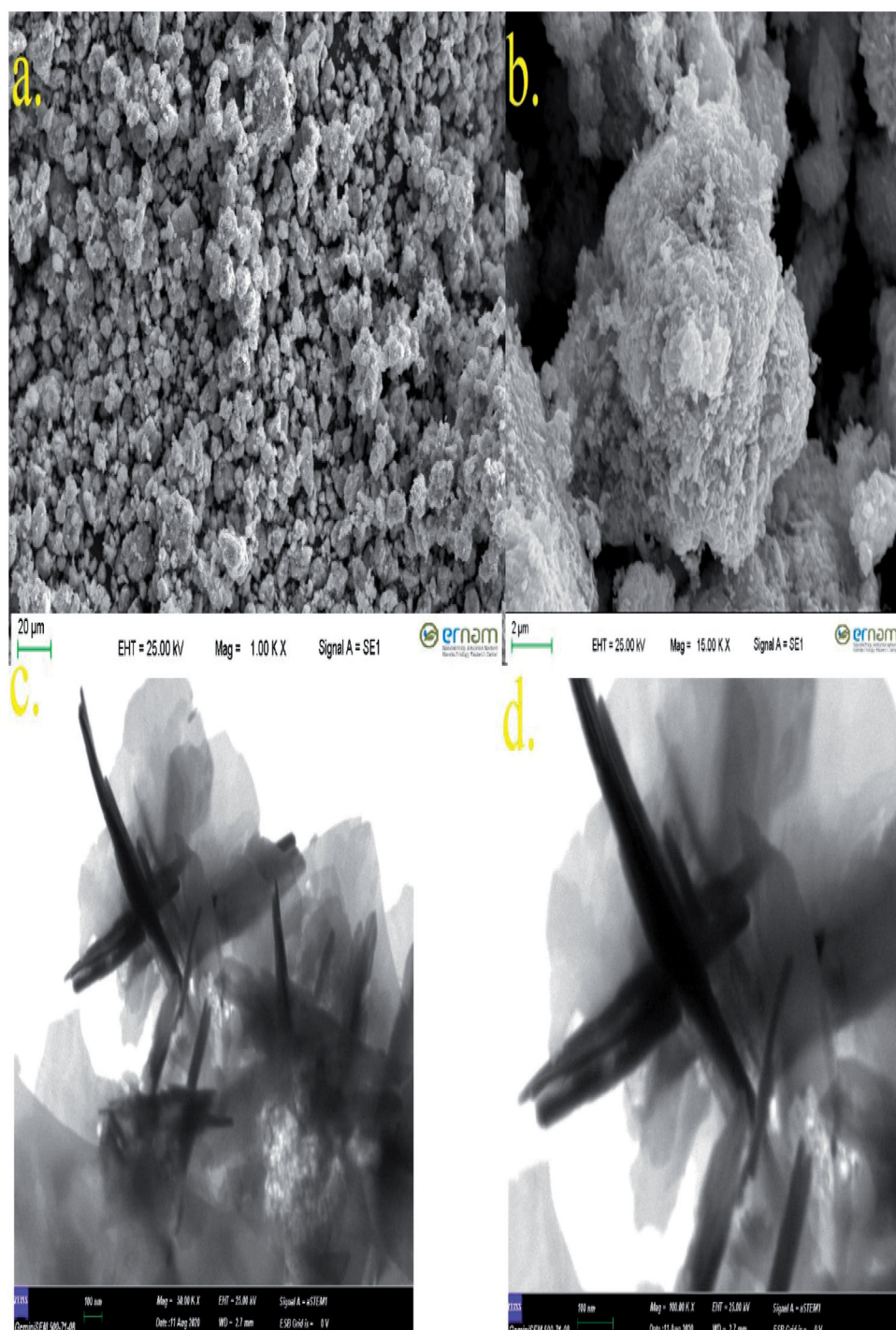
Figure 1. SEM (a,b) and FESEM images (c,d) of CuO NPs (Magnifications: a: 1000×, b: 15,000×, c: 50,000×, and d: 100,000×). The scale bar shows 20 μm (a), 2 μm (b), 100 nm (c), and 100 nm (d).

significant increase in the percentage of apoptotic hemocytes in comparison to the control group ($F = 10.11$, $df = 4$, $p = 0.00$) (Table 4). Force-feeding treatment with 100 and 150 μg CuO NPs caused a significant increase in the percentage of necrotic hemocytes in experimental groups when compared to the control group ($F = 12.61$, $df = 4$, $p = 0.00$) (Table 4). Unlike 24 h results, 72 h results showed that the decrease in the percentage of mitotic hemocytes at 10, 100 and 150 μg were significant when compared to the control group ($F = 9.53$, $df = 4$, $p = 0.00$) (Table 4).

Similar to 24 h results, apoptotic hemocyte percentages increased but these increases were only significant at 100 and 150 μg of CuO NPs when compared to the control group ($F = 18.62$, $df = 4$, $p = 0.00$) (Table 4). A significant 5.86-fold increase was observed in the percentage of necrotic hemocytes at 150 μg ($F = 5.68$, $df = 4$, $p = 0.00$) (Table 4). Finally, 50, 100, and 150 μg of CuO NPs caused a significant increase in the percentage of micronucleated hemocytes in comparison to the control group in 72 h ($F = 8.56$, $df = 4$, $p = 0.00$) (Table 4).

Table 1. XRD peak list of CuO NPs.

Pos. [°2Th.]	Height [cts]	FWHM Left [°2Th.]	d-Spacing [Å]	Rel. int. [%]	Tip width	Matched by
32.50 (1)	68 (6)	0.34 (5)	2.75253	9.22	0.4051	98-002-8662
32.59 (1)	34 (6)	0.34 (5)	2.75253	4.61	0.4051	
35.526 (2)	639 (9)	0.403 (9)	2.52488	87.05	0.4831	98-002-8662
35.618 (2)	320 (9)	0.403 (9)	2.52488	43.52	0.4831	
38.676 (2)	734 (9)	0.456 (8)	2.32620	100.00	0.5477	98-002-8662
38.776 (2)	367 (9)	0.456 (8)	2.32620	50.00	0.5477	
48.763 (6)	160 (5)	0.50 (3)	1.86599	21.85	0.5975	98-002-8662
48.892 (6)	80 (5)	0.50 (3)	1.86599	10.92	0.5975	
53.53 (2)	48 (4)	0.51 (8)	1.71058	6.50	0.6179	98-002-8662
53.67 (2)	24 (4)	0.51 (8)	1.71058	3.25	0.6179	
58.05 (1)	64 (4)	0.59 (7)	1.58767	8.72	0.7043	98-002-8662
58.21 (1)	32 (4)	0.59 (7)	1.58767	4.36	0.7043	
61.562 (9)	108 (6)	0.49 (5)	1.50520	14.68	0.5935	98-002-8662
61.732 (9)	54 (6)	0.49 (5)	1.50520	7.34	0.5935	
66.03 (1)	115 (3)	0.84 (4)	1.41382	15.61	1.0030	98-002-8662
66.21 (1)	57 (3)	0.84 (4)	1.41382	7.81	1.0030	
67.98 (1)	94 (4)	0.62 (4)	1.37789	12.84	0.7463	98-002-8662
68.17 (1)	47 (4)	0.62 (4)	1.37789	6.42	0.7463	
72.12 (3)	28 (3)	0.61 (7)	1.30859	3.81	0.7363	98-002-8662
72.33 (3)	14 (3)	0.61 (7)	1.30859	1.91	0.7363	
75.11 (2)	40 (3)	0.88 (7)	1.26375	5.48	1.0582	98-002-8662
75.33 (2)	20 (3)	0.88 (7)	1.26375	2.74	1.0582	
89.90 (5)	17 (3)	0.6 (2)	1.09028	2.33	0.7671	98-002-8662
90.19 (5)	9 (3)	0.6 (2)	1.09028	1.16	0.7671	
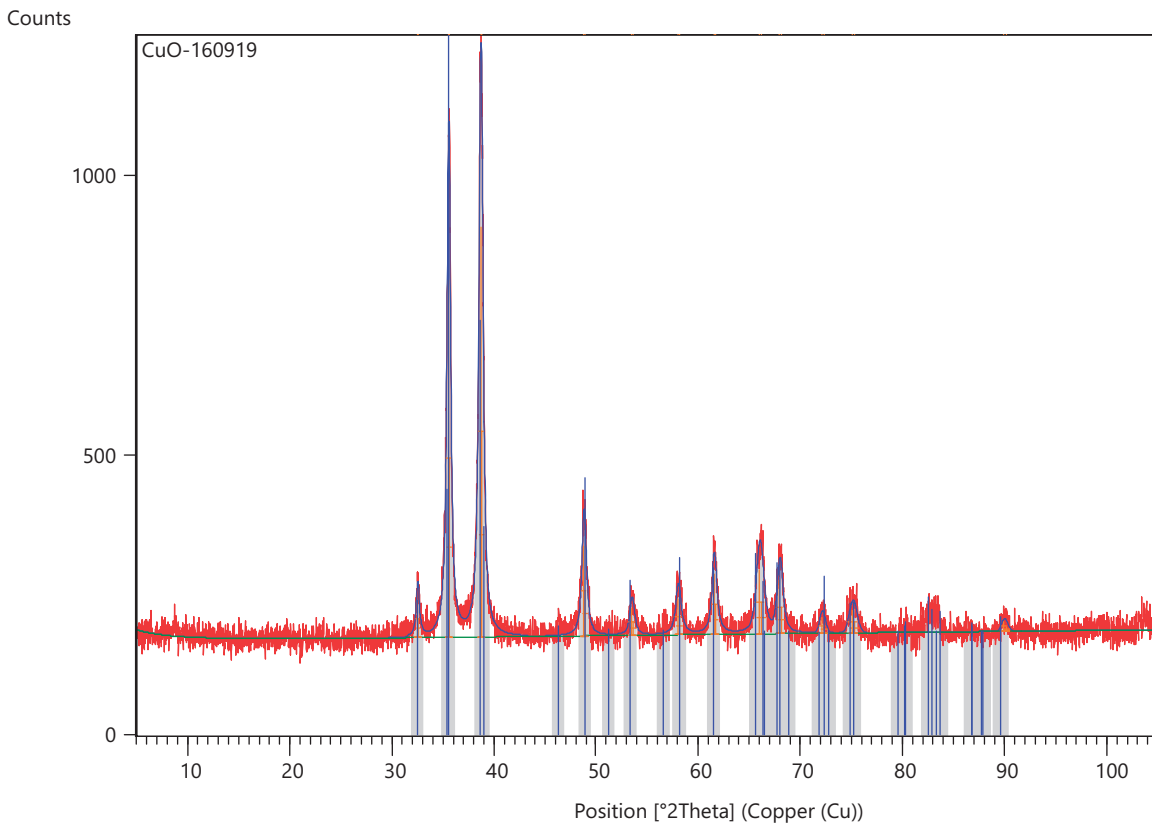
Figure 2. The XRD spectrum of CuO NPs.

Discussion

In this study, we have reported that CuO NPs caused hemocyte fluctuations in larval *G. mellonella* hemolymph as a result of exposure to different concentrations of this chemical. Previous studies showed that TiO_2 NPs (3000 and 5000 ppm) caused a decrease in the number of hemocytes of the last instar larvae of *G. mellonella* (Zorlu *et al*. 2015). 1000, 3000 and 5000 ppm zinc oxide NP (70 nm) decreased significantly the number of hemocytes of the last instar larvae of *G. mellonella* (Nurullahoğlu *et al*. 2015). 24 h post-force-feeding treatment of zinc oxide NP (70 nm) (0.5, 1, 2.5, 5 µg/10 µl) concentrations, the number of hemocytes of *G. mellonella* did not show significant changes in all treatments when compared to the control group but the percentage of the dead cells (10.01%) in the 5 µg/10 µl group was significantly higher than the control group (3.03%) (Eskin *et al*. 2019).

Table 2. Acute 24 and 72 h toxicity experiments of CuO NPs for four instar *G. mellonella* and the estimated LC_{50} and LC_{90} values.

Concentrations of CuO NPs (µg/10 µl)	Mortality and lethal concentration of acute CuO NPs on larvae in 24 h*		Mortality and lethal concentration of acute CuO NPs on larvae in 72 h*	
	Number of exposed larvae*	Number of dead larvae		Number of dead larvae
0 (Control)*	60	0		0
1	60	0		0
10	60	5		7
100	60	33		40
1000	60	57		58
LC_{50} value of acute 24 h toxicity:		370.951 (µg/10 µl), ($y = 0.8 + $2.5E-3*$X$, $R^2 =$ 0.819, Chi-square $= 66.086$, $df = 3$, $p = 0.00$)	LC_{50} value of acute 72 h toxicity:	298.22 (µg/10 µl), ($y = 0.55 + $2.45E-3*$X$, $R^2 =$ 0.784, Chi-square $= 88.790$, $df = 3$, $p = 0.00$)
LC_{90} value of acute 24 h toxicity:		781.709 (µg/10 µl)	LC_{90} value of acute 72 h toxicity:	671.693 (µg/10 µl)

*For all treatments including the control group in 24 and 72 h, the number of larvae was 60.

Tunçsoy and Ozalp (2017) reported that when compared to the control group, the *G. mellonella* larvae given diets with 10 and 100 mg/L of CuO NPs had a significantly higher total hemocyte count (THC), whereas those given 1000 mg/L had a significantly lower THC when compared with the control group. Ibrahim and Ali (2018) proved that the increased number of cells in the circulation of insect hemolymph may result from the NP-derived activation of hematopoietic organs in the silkworm *Spodoptera littoralis* (Lepidoptera: Noctuidae). Another different report dealing with the effects of heavy metals on the endocrine system in insects shows that the reason for the decrease of THC is juvenoid-methoprene in *Papilio demoleus* (Lepidoptera: Papillionidae) (Sendi and Salehi 2010). The researchers noted about this phenomenon could be due to the death of pathological cells by degeneration. But contrariwise, we did not find a significant difference in the total hemocyte count of CuO NPs in treated groups 24 and 72 h post-force-feeding treatment when compared to the control group (Kruskal–Wallis test $p > 0.05$, chi-square $= 7.168$, $p = 0.127$ (24 h), Kruskal–Wallis test $p > 0.05$, chi-square $= 6.736$, $p = 0.151$ (72 h) (Table 3). Although the mitotic index showed a significant increase in 24 h results at 150 µg (Tukey test, $F = 9.75$, $df = 4$, $p = 0.00$) and the mitotic index showed a significant decrease at 72 h results at 10, 100 and 150 µg concentrations (Tukey test, $F = 9.53$, $df = 4$, $p = 0.00$), it was understood that these increase and decrease did not cause a significant change in THCs (Tables 3 and 4). Similarly, Altuntaş *et al*. (2012) showed that GA₃ treatment in *G. mellonella* larvae caused an increase in the mitotic index, but there was no correlation between induced mitotic index and THCs. Duarte *et al*. (2020) reported that stress conditions may not cause an increase or decrease in THCs in insects, which may be due to the duration of the stress period. Fröhlic and Meindl (2015) reported that cytotoxic studies can be performed between 4 and 48 h, but the studies on cellular accumulation or cellular damage of NPs are still insufficient. When different CuO NP exposure periods and different nano-sized CuO NPs are investigated together, various results can be observed on hemocyte counts. Also, heavy metal concentrations can be regulated through feces of insects. Noret *et al*. (2007) found that caterpillars reared on high-zinc leaves regulate their internal zinc concentration through excretion of feces with of high concentration of metals. The regulation of essential metals such as copper and zinc is achieved through the lysis of gut cells (where metals are accumulated) in the lumen of the digestive system for excretion of the feces (Hopkin 1989, Noret *et al*. 2007). In this study, the excretion of CuO NPs from the larval body may have an impact on THCs, hemocyte viability, and mitotic cell percentages in larval hemolymph. DNA damage-induced cell death is executed by apoptosis, necrosis, and mitotic catastrophe. Apoptosis is also the main route of death following DNA damage. Cells undergo apoptosis upon genotoxic stress via the death receptor and/or the intrinsic mitochondrial pathway (Kaina 2011). DNA can be damaged by a variety of exogenous and endogenous insults including chemicals, radiation, free radicals, and topological changes, each causing distinct forms of damage (Curtin 2012, Srinivas *et al*. 2019). Although Cu is a trace element, it can cause cellular reactive oxygen species and apoptosis depend on Cu doses (Panjehpour *et al*. 2010). Raes *et al*. (2000) reported that Cu ($^{2+}$)-induced apoptosis in *Aedes albopictus* (Diptera: Culicidae) C6/36 cell clone cells (2000). They also reported that Cu ($^{2+}$) induced hyper polymerization of the microtubules, cell aggregation, and massive apoptosis. They observed that cell death occured by necrosis when the high doses of Cu were applied to insect. The present study demonstrated that monoclinic 38 nm-sized and flake-like-shaped CuO NPs caused a significant increase in the apoptotic and necrotic index in 24 h and 72 h based on the NP concentrations (Table 4). The reason for the increased apoptotic and necrotic index can be due to molecular mechanisms (DNA damage, ROS molecules, death receptor and/or the intrinsic mitochondrial pathways, etc.), and increased Cu-related ions. CuO NPs can cause chromosomal damage and micronucleus formation (Song *et al*. 2012, Perreault *et al*. 2012, Di Bucchianico *et al*. 2013, Semisch *et al*. 2014). Similarly, in our study, the increase in the percentage of micronucleated hemocytes due to 150 µg of the CuO NPs treatment ($F = 11.76$, $df = 4$, $p = 0.00$) was significant when compared to the control group (Table 4). In addition to this result, 72 h post-force-feeding treatment of the CuO NPs to the larvae, the percentage of micronucleated hemocytes increased at 50, 100, and 150 µg CuO NPs concentrations ($F = 8.56$, $df = 4$, $p = 0.00$) (Table 4). The significant increase in the percentage of micronucleated hemocytes may be due to the chromosomal damages caused by CuO NPs in hemocytes
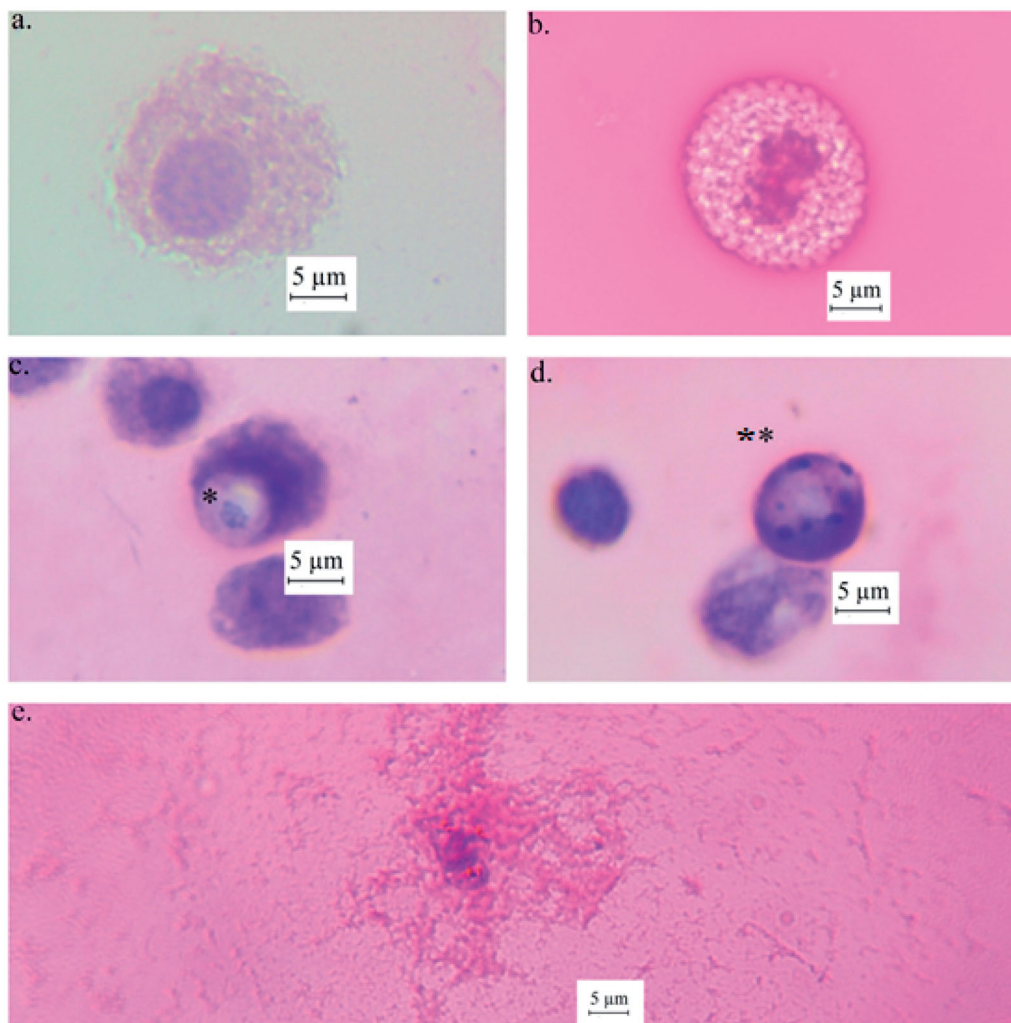
Figure 3. The light microscope images of viable hemocyte-control (a), mitotic hemocyte at 10 µg/10 µl concentration (b), micronucleated hemocyte at 50 µg/10 µl concentration (c), apoptotic hemocyte with apoptotic bodies at 100 µg/10 µl concentration (d), and necrotic hemocyte at 150 µg/10 µl concentration (e). '*' Shows the micronucleus in hemocyte (c) and '**' shows apoptotic hemocyte (d) (1000×). The scale bar shows 5 µm.

Table 3. The mean number of hemocytes counted in Luna cell counting slide and the mean number of hemocytes in 1 ml fourth instar *Galleria mellonella* larva counted by Luna II automated cell counter according to the applied concentrations 24 h and 72 h post-force-feeding treatment.

Concentrations (µg/10 µl)	24 h results		72 h results	
	Hemocyte count (Mean ± SE)*	The number of hemocytes/ml THC × 10⁶ (Mean ± SE)	Hemocyte count (Mean ± SE)*	The number of hemocytes/ml THC × 10⁶ (Mean ± SE)
0	745.46 ± 85.77^{ab}	17.72 ± 1.71^{ab}	692.86 ± 73.93^{ab}	16.32 ± 1.71^{ab}
10	699.60 ± 92.72^{a}	16.80 ± 4.41^{a}	1036.86 ± 190.16^{b}	24.40 ± 4.41^{b}
50	839 ± 103.64^{ab}	19.40 ± 2.21^{ab}	916.13 ± 92.10^{b}	21.96 ± 2.21^{b}
100	998 ± 102.9^{b}	23.72 ± 3.15^{b}	869.66 ± 137.54^{ab}	21.16 ± 3.15^{ab}
150	979.93 ± 135.46^{ab}	23.20 ± 2.53^{ab}	617.33 ± 58.02^{a}	14.96 ± 2.53^{a}
	Mann–Whitney U-test, p	0.00	Mann–Whitney U-test, p	0.00
	F	7.16	F	5.74
	df	4	df	4

*Data are means ± standard errors of three replicates carried out with five larvae per replicate. Different letters in the same vertical column showed significant differences within different concentrations (Mann–Whitney U-test, $p < 0.05$).

(Song *et al.* 2012, Perreault *et al.* 2012, Di Bucchianico *et al.* 2013, Semisch *et al.* 2014). Baršienė *et al.* (2010) found in *Mytilus edulis* that the frequency of micronuclei (MN/1000 cells) varied from 0.65% to 3.35%, of nuclear buds (NB/1 000 cells) – from 1.85% to 3.40%, of fragmented-apoptotic cells (FA/1 000 cells) from 0.95% to 3.25%, of bi-nucleated cells (BN/1 000 cells) from 1.75% to 2.90% when mussels inhabiting northern Atlantic zones were impacted by contaminated

aluminum industry sites. The percentage values seen in Baršienė *et al.* (2010) are compatible with the values in our study (Table 4). Consequently, our results showed that when CuO NPs are taken directly into the insect larval body by a force-feeding method with 10–150 µg concentrations, CuO NPs caused significant fluctuations in mitotic hemocyte ratios, increased the apoptotic and necrotic hemocyte ratios, and caused micronucleated hemocytes in 24 and 72 h. In addition

Table 4. Percentages of viable, mitotic, apoptotic, necrotic, and micronucleated cells of *Galleria mellonella* larvae during 24 h and 72 h post-force-feeding treatment.

CuO NP concentrations (μg/10 μl)	Viable cells (%)*	Mitotic cells (%)*	Apoptotic cells (%)*	Necrotic cells (%)*	Micronucleated cells (%)*
24 h results					
0	96.89[a]	1.47[a]	0.57[a]	0.67[a]	0.40[a]
10	96.76[a]	1.15[a]	0.70[a]	0.89[ab]	0.48[a]
50	94.34[b]	1.62[a]	2.09[b]	0.90[ab]	1.04[a]
100	93.28[bc]	0.90[a]	2.10[b]	2.78[c]	0.92[a]
150	91.40[c]	2.78[b]	2.45[b]	1.36[b]	1.99[b]
p (Tukey test)	0	0	0	0	0
F	13.86	9.75	10.11	12.61	11.76
df	4	4	4	4	4
72 h results					
0	97.94[a]	1.01[ab]	0.35[a]	0.30[a]	0.38[a]
10	97.63[a]	0.52[c]	0.62[a]	0.66[ab]	0.55[a]
50	95.74[b]	1.57[a]	1.07[ab]	0.56[a]	1.04[b]
100	94.44[bc]	0.97[bc]	1.85[b]	0.64[a]	2.08[c]
150	92.48[c]	0.71[bc]	3.52[c]	1.76[b]	1.50[c]
p (Tukey test)	0	0	0	0	0
F	20.21	9.53	18.62	5.68	8.56
dF	4	4	4	4	4

*Data are means ± standard errors of three replicates using five larvae per replicate. Different letters in the same vertical column indicated significant differences within different concentrations (Mann–Whitney U-test, $p < 0.05$).

to these results, it was understood that CuO NPs did not change the THCs significantly when *G. mellonella* larvae were exposed to 10, 50, 100, and 150 μg CuO NPs 24 and 72 h post-force-feeding treatment. The present *in vivo* study was designed to investigate the effects of CuO NPs under different biological parameters with particular focus on such as toxicity, hemocyte viability, and hemocyte density in the hemolymph in an insect species *G. mellonella*. Although our knowledge on the toxicity of various CuO NPs in the living organisms has increased over the past few years, there is still a lack of knowledge regarding exposure concentrations, toxicologic effects of CuO NPs on the insect innate immune system, as well as LC_{50} and LC_{90} values which could potentially affect their toxicity. In this context, this paper is centering on the effects of the most commonly used and commercially available CuO NP using *G. mellonella* as a model experiment species. *In vivo* evaluation studies with NPs on model experiment organisms have been providing information to support a better understanding about the interactions of nanoscale materials with biological systems.

Conclusion

Nowadays, the application of NPs in the field of insect pest management is very important. It is necessary to find out the adverse effects of NPs on insect species. In conclusion, we have studied the toxic effects of the 38 nm sized and flake-like shaped CuO NPs on insects, using *G. mellonella* as a model organism. Our study suggests that CuO NPs caused alterations to the THCs, caused significant changes in the percentages of viable, mitotic, apoptotic, necrotic, and micronucleated hemocytes. Finally, the toxicity values ($LC_{50–90}$) of 38 nm sized and flake-like-shaped CuO NPs on *G. mellonela* were also determined for the first time with this study.

ORCID

A. Eskin (iD) http://orcid.org/0000-0002-7953-654X
Hakan Bozdoğan (iD) http://orcid.org/0000-0002-6836-4383

References

Alarifi, S., *et al.*, 2013. Cytotoxicity and genotoxicity of copper oxide nanoparticles in human skin keratinocytes cells. *International Journal of Toxicology*, 32 (4), 296–307.
Altuntaş, H., *et al.*, 2012. Effects of gibberellic acid on hemocytes of *Galleria mellonella* L. (Lepidoptera: Pyralidae). *Environmental Entomology*, 41 (3), 688–696.

Altuntaş, H., et al., 2016. Etefonun model organizma Galleria mellonella L. 1758 (Lepidoptera: Pyralidae) üzerine toksikolojik ve fizyolojik etkileri. Türkiye Entomoloji Dergisi, 40 (4), 413–423.

Andrea, A., Krogfelt, A.K., and Jenssen, H., 2019. Methods and challenges of using the greater wax moth (Galleria mellonella) as a model organism in antimicrobial compound discovery. Microorganisms, 7 (3), 85–89.

Baršienė, J., et al., 2010. Environmental genotoxicity and cytotoxicity studies in mussels and fish inhabiting northern Atlantic zones impacted by aluminum industry. Ekologija, 56 (3), 116–123.

Beaulaton, J., 1979. Hemocytes and hemocytopoiesis in silkworms. Biochimie, 61 (2), 157–164.

Bolognesi, C., 2019. Micronucleus experiments with bivalve mollusks. In: S. Knasmüller and M. Fenech, eds. The micronucleus assay in toxicology. London: Royal Society of Chemistry, Chapter 17, 273–289.

Bouazizi, N., et al., 2015. Effect of synthesis time on structural, optical and electrical properties of CuO nanoparticles synthesized by reflux condensation method. Advanced Materials Letters, 6 (2), 158–164.

Brandelli, A., 2020. The interaction of nanostructured antimicrobials with biological systems: cellular uptake, trafficking and potential toxicity. Food Science and Human Wellness, 9 (1), 8–20.

Chikkanna, M.M., Neelagund, S., and Hiremath, M.B., 2018. Biological synthesis, characterization and antibacterial activity of novel copper oxide nanoparticles (CuONPs). Journal of Bionanoscience, 12 (1), 92–99.

Curtin, J.N., 2012. DNA repair dysregulation from cancer driver to therapeutic target. Nature Reviews. Cancer, 12 (12), 801–817.

Dere, B., Altuntaş, H., and Nurullahoğlu, U.Z., 2015. Insecticidal and oxidative effects of azadirachtin on the model organism Galleria mellonella L. (Lepidoptera: Pyralidae). Archives of Insect Biochemistry and Physiology, 89 (3), 138–152.

Dere, B., Nurullahoğlu, U.Z., and Altuntaş, H., 2019. Effects of azadirachtin on development of model insect Galleria mellonella L. (Lepidoptera: Pyralidae). Eskişehir Teknik Üniversitesi Bilim ve Teknoloji Dergisi C-Yaşam Bilimleri ve Biyoteknoloji, 8 (1), 85–91.

Dhawan, A., and Sharma, V., 2010. Toxicity assessment of nanomaterials: methods and challenges. Analytical and Bioanalytical Chemistry, 398 (2), 589–605.

Di Bucchianico, S., et al., 2013. Multiple cytotoxic and genotoxic effects induced in vitro by differently shaped copper oxide nanomaterials. Mutagenesis, 28 (3), 287–299.,

Duarte, J.P., et al., 2020. Do dietary stresses affect the immune system of Periplaneta americana (Blattaria: Blattidae)? Brazilian Journal of Biology, 80 (1), 73–78. , ISSN 1519-6984, On-line version, DOI: http://dx.doi.org/10.1590/1519-6984.190035.

Eltarahony, M., Zaki, S., and Abd-El-Haleem, D., 2018. Concurrent synthesis of zero-and one-dimensional, spherical, rod-, needle-, and wire-shaped CuO nanoparticles by Proteus mirabilis 10B. Journal of Nanomaterials, 2018, 1–14.

Eskin, A., Öztürk, Ş., and Körükçü, M., 2019. Determination of the acute toxic effects of zinc oxide nanoparticles (ZnO NPs) in total hemocytes counts of Galleria mellonella (Lepidoptera: Pyralidae) with two different methods. Ecotoxicology, 28 (7), 801–808.

Eskin, A., et al., 2020. Fluorescent copper phosphate nanoflowers: a novel toxicity investigation study based on Tenebrio Molitor Linnaeus, 1758 (Coleoptera: Tenebrionidae) larvae. Bitlis Eren Üniversitesi Fen Bilimleri Dergisi, 9 (3), 975–984.

Ferri, K.F., and Kroemer, G., 2001. Organelle-specific initiation of cell death pathways. Nature Cell Biology, 3 (11), E255–263.

Foley, S. (2018) Metal-organic materials as electrode precursors and host for lithium-ion and lithium-sulfur batteries. Doctoral thesis. The University of Limerick, Department of Chemical Sciences, 1–268.

Fröhlich, E., and Meindl, C., 2015. In vitro assessment of chronic nanoparticle effects on respiratory cells. In: M.L. Larramendy and S. Soloneski, eds. Nanomaterials, toxicity and risk assessment. London: Intech Open, Chapter 4, 69–92.

Gwokyalya, R., and Altuntaş, H., 2019. Boric acid-induced immunotoxicity and genotoxicity in model insect Galleria mellonella L. (Lepidoptera: Pyralidae)). Archives of Insect Biochemistry and Physiology, 101 (4), e21588.

Hasan, S., 2015. A review on nanoparticles: their synthesis and types. Research Journal of Recent Sciences, 4, 9–11.

Hassan, K.H., Al-Bayati, T.H.M., and Abbas, Z.M.A., 2012. Study and characterization of copper oxide nanoparticles prepared by chemical method using X-ray diffraction and scanning electron microscope. American Journal of Scientific Research, 77, 49–53.

Hayashi, M., 2016. The micronucleus test-most widely used in vivo genotoxicity test. Genes Environ, 38, 18.

Hopkin, S. P., 1989. Ecophysiology of metals in terrestrial invertebrates. Amsterdam: Elsevier Applied Science Publishers.

IBM-SPSS Statistics for Windows. 2011. Version 20.0. Elsevier, London, UK. IBM Corp. Released. Armonk, NY: IBM Corp.

Ibrahim, A.M.A., and Ali, M.A., 2018. Silver and zinc oxide nanoparticles induce developmental and physiological changes in the larval and pupal stages of Spodoptera littoralis (Lepidoptera: Noctuidae). Journal of Asia-Pacific Entomology, 21 (4), 1373–1378.

Istifli, E.S., Hüsunet, M.T., and Ila, H.B., 2019. Cell division, cytotoxicity, and the assays used in the detection of cytotoxicity. In: E. Salih Istifli and H. Basri İla, eds. Cytotoxicity-definition, identification, and cytotoxic compounds. London: Intech Open, 1–19.

Jeevanandam, J., et al., 2018. Review on nanoparticles and nanostructured materials: history, sources, toxicity and regulations. Beilstein J Nanotechnol, 9 (1), 1050–1074.

Kaina, B., 2011. DNA damage-induced apoptosis. In: M. Schwab, ed. Encyclopedia of cancer. Berlin, Heidelberg: Springer.

Keller, A.A., et al., 2017. Comparative environmental fate and toxicity of copper nanomaterials. NanoImpact, 7, 28–40.

Koç-Başer, D., et al., 1999. Spontaneous micronuclei in cytokinesis-blocked bone marrow and peripheral blood lymphocytes of CML patients. Turkish Journal of Medical Sciences, 29, 125–128.

Luo, C., et al., 2014. Activation of Erk and p53 regulates copper oxide nanoparticle-induced cytotoxicity in keratinocytes and fibroblasts. International Journal of Nanomedicine, 9, 4763–4772.

Mukherji, S., et al., 2019. Synthesis and characterization of size-and shape-controlled silver nanoparticles. Physical Sciences Reviews, 4 (1), 20170082.

Nakamura, S., et al., 2019. Synthesis and application of silver nanoparticles (Ag NPs) for the prevention of infection in healthcare workers. International Journal of Molecular Sciences, 20 (15), 3620.

Nayak, A., et al., 2016. Histochemical detection and comparison of apoptotic cells in the gingival epithelium using hematoxylin and eosin and methyl green-pyronin: a pilot study. Journal of Indian Society of Periodontology, 20 (3), 294–298.

Neuwirth, M., 1973. The structure of the hemocytes of Galleria mellonella (Lepidoptera). Journal of Morphology, 139 (1), 105–123.

Noret, N., et al., 2007. Development of Issoria lathonı a (Lepidoptera: Nymphalidae) on zinc-accumulating and nonaccumulating Viola species (Violaceae). Environmental Toxicology and Chemistry, 26 (3), 565–571.

Nurullahoğlu, U.Z., Eskin, A., Kaya, S., 2015. Effects of zinc oxide nanoparticles on hemocytes of Galleria mellonella (L.) (Lepidoptera: Pyralidae). International conference on civil and environmental engineering, May 20–23, Cappadocia, Nevsehir, Turkey, 392.

Oberdorster, G., Oberdorster, E., and Oberdorster, J., 2005. Nanotoxicology: an emerging discipline evolving from studies of ultrafine particles. Environmental Health Perspectives., 113, 823–839.

Ou, Y., et al., 2014. Molecular mechanisms of exopolysaccharide from Aphanothece halaphytica (EPSAH) induced apoptosis in hela cells. PLoS One, 9 (1), e87223

Panjehpour, M., Taher, M.A., and Bayestesh, M., 2010. The growth inhibitory effects of cadmium and copper on the MDA-MB468 human breast cancer cells. Journal of Research in Medical Sciences, 15 (5), 279–286. PMID: 21526096.

Pereira, T.C., et al., 2018. Recent advances in the use of Galleria mellonella model to study immune responses against human pathogens. Journal of Fungi, 4 (4), 128, DOI:.

Perreault, F., et al., 2012. Genotoxic effects of copper oxide nanoparticles in neuro 2A cell cultures. Science of the Total Environment, 441, 117–124.

Pfaller, T., *et al.*, 2010. The suitability of different cellular in vitro immuno-toxicity and genotoxicity methods for the analysis of nanoparticle-induced events. *Nanotoxicology*, 4 (1), 52–72.

Quirino, R.M., *et al.*, 2018. CuO rapid synthesis with different morphologies by the microwave hydrothermal method. *Materials Research*, 21 (6), e20180227.

Raes, H., *et al.*, 2000. Copper induces apoptosis in *Aedes* C6/36 cells. *The Journal of Experimental Zoology*, 1, 286 (1), 1–12.

Rahman, A., *et al.*, 2017. Post embryonic development of *Galleria mellonella* L. and its management strategy. *Journal of Entomology and Zoology Studies*, 5, 3, 1523–1526.

Rai, M., *et al.*, 2015. Bioactivity of noble metal nanoparticles decorated with biopolymers and their application in drug delivery. *International Journal of Pharmaceutics*, 496 (2), 159–172. 10.1016./j.ijpharm.2015.10.059.

Ramarao, N., Nielsen-Leroux, C., and Lereclus, D., 2012. The insect *Galleria mellonella* as a powerful infection model to investigate bacterial pathogenesis. *Journal of Visualized Experiments*, 70 (70), 4392.

Reddy, S., Swamy, B.K., and Jayadevappa, H., 2012. CuO nanoparticle sensor for the electrochemical determination of dopamine. *Electrochimica Acta*, 61, 78–86.

Richardson, R.T., *et al.*, 2018. Morphological and functional characterization of honey bee, *Apis mellifera*, hemocyte cell communities. *Apidologie*, 49 (3), 397–410.

Sahdan, M.Z., *et al.*, 2015. Fabrication and characterization of crystalline cupric oxide (CuO) films by simple immersion method. *Procedia Manufacturing*, 2, 379–384.

Sahu, C.S., and Hayes, W.A., 2017. Toxicity of nanomaterials found in human environment: a literature review. *Toxicology Research and Application*, 1, 239784731772635–239784731772613.

Semisch, A., *et al.*, 2014. Cytotoxicity and genotoxicity of nano- and microparticulate copper oxide: role of solubility and intracellular bio-availability. *Particle and Fibre Toxicology*, 11, 10–16.

Sendi, J., and Salehi, R., 2010. The effect of methoprene on total hemocyte counts and histopathology of hemocytes in *Papilio demoleus* (Lepidoptera). *Munis Entomology and Zoology*, 5 (1), 240–246.

Shafagh, M., Rahmani, F., and Delirezh, N., 2015. CuO nanoparticles induce cytotoxicity and apoptosis in human K562 cancer cell line via mitochondrial pathway, through reactive oxygen species and P53. *Iranian Journal of Basic Medical Sciences*, 18 (10), 993–1000.

Shaffiey, S.F., *et al.*, 2014. Synthesis and evaluation of bactericidal properties of CuO nanoparticles against *Aeromonas hydrophila*. *Nanomedicine Journal*, 1 (3), 198–204.

Simon, H.U., Haj-Yehia, A., and Levi-Schaffer, F., 2000. Role of reactive oxygen species (ROS) in apoptosis induction. *Apoptosis*, 5 (5), 415–418.

Simonin, M., *et al.*, 2018. Negative effects of copper oxide nanoparticles on carbon and nitrogen cycle microbial activities in contrasting agricultural soils and in presence of plants. *Frontiers in Microbiology*, 9, 3102. DOI:.

Srinivas, U.S., *et al.*, 2019. ROS and the DNA damage response in cancer. *Redox Biology*, 25, 101084.

Song, M.F., *et al.*, 2012. Metal nanoparticle-induced micronuclei and oxidative DNA damage in mice. *Journal of Clinical Biochemistry and Nutrition*, 50 (3), 211–216.

Tomanin, R., *et al.*, 1991. Influence of smoking habit on the frequency of micronuclei in human lymphocytes by the cytokinesis block method. *Mutagenesis*, 6 (2), 123–126.

Tran, T.H., and Nguyen, V.T., 2014. Copper oxide nanomaterials prepared by solution methods, some properties, and potential applications: a brief review. *International Scholarly Research Notices*, 2014, 856592

Tunçsoy, B.S., and Ozalp, P., 2017. Effects of copper oxide nanoparticles on hemocytes of *Galleria mellonella*. *Toxicology Letters*, 280, S187.

Tunçsoy, S.B., 2018. Toxicity of nanoparticles on insects. *Adana Science and Technology University*, 1 (2), 49–61.

Tunçsoy, S.B., *et al.*, 2019. Effects of copper oxide nanoparticles on tissue accumulation and antioxidant enzymes of *Galleria mellonella* L. *Bulletin of Environmental Contamination and Toxicology*, 102 (3), 341–346.

Venier, P., Maron, S., and Canova, S., 1997. Detection of micronuclei in gill cells and haemocytes of mussels exposed to benzo[a]pyrene. *Mutation Research/Genetic Toxicology and Environmental Mutagenesis*, 390 (1-2), 33–44.

Vieira, A.F.C., and Silveria, L.G., 2018. Cyto(geno)toxic endpoints assessed via cell cycle bioassays in plant dodels. *In:* T.A. Çelik, ed. *Cytotoxicity*. London: Intech Open, 117–129.

Yankson, A.A., *et al.*, 2019. A low cost synthesis and characterization of CuO nanoparticles for photovoltaic applications. *Ghana Journal of Science*, 60 (1), 17–23.

Yang, H., *et al.*, 2009. Comparative study of cytotoxicity, oxidative stress and genotoxicity induced by four typical nanomaterials: the role of particle size, shape and composition. *Journal of Applied Toxicology*, 29 (1), 69–78.,

Zhang, L., *et al.*, 2014. In situ study of thermal stability of copper oxide nanowires at anaerobic environment. *Journal of Nanomaterials*, 2014, 1–6.

Zorlu, T., Nurullahoğlu, U.Z., and Kaya, S., 2015. Effects of titanium nanoparticles on hemocytes of *Galleria mellonella* (L.) (Lepidoptera: Pyralidae). *International conference on civil and environmental engineering*, May 20–23, Cappadocia, Nevsehir, Turkey, 393.

Zorlu, T., Nurullahoğlu, U.Z., and Altuntaş, H., 2018. Influence of dietary titanium dioxide nanoparticles on the biology and antioxidant system of model insect, *Galleria mellonella* (L.) (Lepidoptera: Pyralidae). *Journal of the Entomological Research Society*, 20 (3), 1–15.